Time scales of regional circulation of saline fluids in continental crystalline rock aquifers (Armorican massif, Western France)

Submitted to HESS (April 2014)

A. ARMANDINE LES LANDES[1*], L. AQUILINA[1], P. DAVY[1], V. VERGNAUD-AYRAUD[1], C. LE CARLIER[1]

[1] *Geosciences Rennes (CNRS - UMR 6118)*
University of Rennes 1
Bâtiment 14B
Campus Beaulieu
263 Avenue du Général Leclerc
35042 Rennes
France

[*]*antoine.armandineleslandes@univ-rennes1.fr, (+33) 223 23 66 24*

luc.aquilina@univ-rennes1.fr

philippe.davy@univ-rennes1.fr

virginie.vergnaud@univ-rennes1.fr

christian.le-carlier@univ-rennes1.fr

[*]Corresponding author

ABSTRACT

In recent decades, saline fluids have been sampled worldwide at great depths in continental basements. Although some of them have been attributed to marine transgressions the mechanisms allowing their circulation is not understood. In this paper, we describe the horizontal and vertical distribution of moderately saline fluids (60 to 1400mg/l) sampled at depths ranging from 41m to 200m in crystalline rock aquifers at the regional scale of the Armorican Massif (northwestern France). The horizontal and vertical distributions of high chloride concentrations are in good agreement with both the altitudinal and vertical limits and succession of the three major transgressions between the Mio-Pliocene and Pleistocene ages. The mean chloride concentration for each transgression area is exponentially related to the time spanned until present. It defines the potential laws of leaching (displacement) of marine waters by fresh meteoric waters. The results of the Armorican aquifers provide the first observed constraints for the time scales of seawater circulation in the continental crystalline basement and the subsequent leaching by fresh meteoric waters. The general trend of increasing chloride concentration with depth and the time frame for the flushing process provide useful information to develop conceptual models of the paleo-functionning of Armorican aquifers.

Highlights:

- **The Armorican massif presents clear evidences of a marine origin of the saline component in the fluids at the regional scale.**

- **High chloride concentrations are attributed to three past marine transgressions.**

- **Saline fluids provide constraints for the time scales of fluid circulation.**

50 • **The general trend of increasing chloride concentration with depth supports the**

51 **seawater introduction by gravity-driven flow at depth in the basement.**

52 • **The time frame for the flushing process is useful information to develop**

53 **conceptual models of the paleo-functioning of Armorican aquifers.**

1. INTRODUCTION

In recent decades, saline fluids have been sampled at great depths (0.5 - 5 km) in continental basements (Bucher and Stober, 2010; Frape et al., 2003). In several places, these fluids have been considered as old seawater introduced in aquifers during marine transgressions (Aquilina and Dreuzy, 2011; Beaucaire et al., 1999; Bottomley et al., 1994, 1999; Douglas et al., 2000; Greene et al., 2008; Louvat et al., 1999; Négrel and Casanova, 2005). Two alternative origins related either to glacial recharge of brines due to cryogenic mechanisms (Starinsky and Katz, 2003), or to anthropogenic sources (Kelly et al., 2008; Mullaney et al., 2009; Panno et al., 2006; Perera et al., 2013) have also been proposed. These three hypotheses have led to extremely different estimates of the saline fluid residence time (Devonian or Pleistocene for the Canadian brines, for example) and thus of the paleohydrogeology of the continental aquifers. Although thorough investigations have been carried out in several places, the origin and fate of the salinity are still issues. We have almost no field observations identifying the potential mechanisms leading to marine fluid introduction and conservation in hard rock aquifers, as well as the influence of glacial recharge at various depths in these aquifers remain. Furthermore, the time-scales of these mechanisms are unknown.

In this study, we investigated the effects of marine transgressions in the spatial (both horizontal and vertical) distribution of chloride concentrations at a regional scale. Since the transgression characteristics differ from one event to another, we expect to find higher concentrations in the areas flooded by the later. The decrease of chloride concentrations with time potentially provides constraints for fluid circulation time-scales in the basement. This concept is based on the fact that during transgression, a large amount of chlorides was introduced in flooded areas. Secondly, the chloride concentration of the submerged area decreases under the influence of dilution/leaching by meteoric waters. Thus, the decline in chloride concentration since the time of the last transgression is characteristic of the

The study focuses on the Armorican basement (western France), where several authors have
reported evidence of saline fluids (Ayraud et al., 2008; Pauwels et al., 2010). Three main
transgressions were recorded during Mio-Pliocene to Pleistocene times, the latest being the
highest. This is a particularly favorable context since a large part of the area flooded by the
oldest and highest transgression remains unaffected by later transgression events.

2. GEOLOGICAL BACKGROUND

The Armorican basement extends over an area of 68,500 km² in the northwestern part of
France. The Armorican massif is a crystalline basement localized between the English
Channel and the Bay of Biscay. The northern part corresponds to the Cadomian orogenic belt
(Chantraine et al., 2001). The central and southern zones belong to the European Variscan belt
(Le Corre et al., 1991). The Armorican massif is a basement made of Upper Proterozoic to
Paleozoic formations mainly composed of low and high metamorphic rocks (schists,
sandstones and gneisses…), plutonic (granite) and volcanic (basalt) rocks deformed during
the two orogenies (Cadomian and Variscan) (Fig. 1). These orogenies have initially developed
the main tectonic structures of the Armorican massif: the North and the South Armorican
Shear Zones (NASZ and SASZ, respectively), and the Quessoy/Nort-sur-Erdre Fault (Bonnet
et al., 2000) (Fig. 1). These structures have been reactivated during Mesozoic and Cenozoic
periods. Tertiary and quaternary geodynamic evolution of the Armorican massif are related to
the collision between Europe and Africa (Brault, 2002; Gros and Limasset, 1984; Ziegler,
1990). This evolution mainly consists in three major steps (Thomas, 1999): (1) From the end
of Cretaceous to the upper Eocene, the Armorican massif is subjected to a lithospheric
buckling due to the Pyrenean compression. (2) From the upper Eocene to Oligocene the

103 buckling decreases and the geodynamic evolution is driven by a generalized extension. (3)

104 From the Mio-Pliocene to present days, the Armorican massif is uplifted due to a lithospheric

105 buckling in relation with the Alpine compression. This compression is still active as observed

106 through the Armorican massif seismic activity (Lenôtre et al., 1999; Nicolas et al., 1990).

107 Local topography is controlled by rock lithologies and, on a larger scale, by tectonic faults

108 (Northern and southern shear zones (Dugué, 2007; Gumiaux et al., 2004)). It is relatively

109 moderate with three domains of higher elevation above 200m and a maximum elevation of

110 416m in the east (Fig. 2).

111 **3. HYDROGEOLOGICAL SETTING**

112 The main groundwater flow in crystalline rock aquifers is considered to be localized in

113 superficial formations resulting mainly from rock weathering, and below in fracture and

114 major geologic discontinuities networks (Larsson, 1987; Stober and Bucher, 2007; Wyns et

115 al., 2004). The compartmentalized structure includes various reservoir scales and

116 characteristic physical parameters (permeability, porosity…) varying over several orders of

117 magnitude (Clauser, 1992). At the scale of the Armorican massif a weathered layer 20 to 30m

118 thick is present in many places, and likely ubiquitously (Brault, 2002; Dewandel et al., 2006).

119 Roques (2013) has studied the influence of fault zones for sites characterized by high

120 groundwater yields at the scale of the Armorican massif. At this scale, groundwater resources

121 in the shallower part (<20m) are widespread but limited in term of productivity. Conversely,

122 high groundwater productivities are associated to fault zones below the weathered zone.

123 Indeed, groundwater resources at significant depth have been found in the Armorican bedrock

124 (Le Borgne et al., 2006; Leray et al., 2013; Roques et al., 2014) and it can be considered that

125 the fractured system constitutes a water reservoir in the continental basement. Free

126 groundwater circulation in crystalline environments has been reported from several studies

127 (Banks et al., 1996; Larsson, 1987). Several studies have shown that basement is generally

128 characterized by an interconnected fracture system at several km depth (Aquilina and Dreuzy,

129 2011; Edmunds and Savage, 1991; Stober et al., 2002). Hydrodynamic properties of

130 crystalline rock aquifers of the Armorican basement have been intensively investigated in

131 several research sites (Ploemeur and St-Brice-en-Cogles sites, Fig. 2) (Le Borgne et al., 2004,

132 2006; Dorn et al., 2012; Leray et al., 2013; Roques, 2013; Roques et al., 2014; Touchard,

133 1999) (Fig. 2). Moreover, previous studies in the Armorican basement have identified a

134 compartmentalization of these crystalline rock aquifers from hydrological, geochemical,

135 geological and geophysical data (Ayraud et al., 2008; Roques, 2013; Roques et al., 2014), and

136 from regional-scale numerical modeling (Goderniaux et al., 2013). Geochemical studies also

137 showed specific chemical compositions of the water in the deep fractured aquifer, potentially

138 including saline groundwaters (Aquilina et al., 2013; Ayraud et al., 2008; Pauwels et al.,

139 2013).

140 **4. CHLORIDE DATABASE**

141 The quantity supplied and the quality of the main groundwater resources in the Armorican

142 massif are monitored through a public well network (ADES: "banque nationale d'Accès aux

143 Données sur les Eaux Souterraines", National database for groundwater resources,

144 http://www.ades.eaufrance.fr/). For most of these wells hydrogeological informations

145 (geographical location, altitude, depth, drilling log, borehole parameters, water inflow points,

146 etc…) are available through a second public database of drillings (BSS: "Base de données du

147 Sous-Sol", http://infoterre.brgm.fr/). The precise location of water inflows is not described for

148 each well, and it has been considered that the water inflow corresponds to the base of the well.

149 This assumption is valid taking into account the drilling goal which is to stop the well drilling

150 when a sufficient water inflow is found.

151 The network of wells investigated covers the whole Armorican basement and includes more

152 than 1800 drillings with an average depth of approximately 40m. Chemical records, such as

153 chloride or nitrate concentrations, are available for each drilling. We first preprocessed the

154 database of 1874 chloride measurements and removed wells that are potentially not

155 representative of natural chloride concentrations. We removed wells close to a potential

156 anthropic pollution source (industrial estate, garbage dump, mill pond…), and wells with a

157 large variability through time large (standard deviation of chloride concentration higher than

158 30%). We also did not consider the wells at a distance less than one kilometer from the

159 current coastline, whose concentration may be directly influenced by current saltwater

160 intrusion. 716 of the 1874 wells have been excluded from the database, i.e. 38% of the total.

161 The vertical distribution of the chloride concentrations for the remaining values was analyzed

162 by intervals of 10m from an altitude of 350m above sea level to -125m. The average chloride

163 concentration and the 90th percentile were calculated for each 10m interval.

164   5.   MARINE TRANSGRESSION CHARACTERISTICS

165 Chlorides of marine origin that are not brought by rainfall (i.e. concentrations higher than

166 40 mg.l^{-1}) are likely related to marine transgressions that flooded the Armorican massif from

167 times to times. The likely scenario is that a fairly large amount of chlorides is injected during

168 each transgression in submerged regions, and that the salt concentration decreases from the

169 end of the transgression event due to dilution or leaching by meteoric waters. If the

170 leaching/dilution is efficient enough, for instance if the time lag between two successive

171 transgressions is larger than the leaching time, the system is fully reset by the last event (i.e.

172 the amount of chloride injected during the last event is much larger than the residual of

173 formers). The objective of this part is to characterize the last transgressions that have flooded

174 the Armorican massif.

175 According to stratigraphic record studies in the Armorican Massif and, to the eustatic sea-

176 level fluctuations (Hardenbol et al., 1998), three main transgressions can be identified since

177 the Mio-Pliocene. The oldest of Messinian age has been identified in several places

178 (Néraudeau et al., 2003; Van Vliet-Lanoe et al., 1998), and dated between 6 and 4.6 Myr by

179 several methods (ESR: Electron Spin Resonance Spectroscopy on quartz, $^{87}Sr/^{86}Sr$ on shells

180 and bones in "Redonian" shelly sands or "Faluns" (Mercier et al., 2000; Néraudeau et al.,

181 2002). These sediments would attest of the maximum transgression of the late Neogene in

182 northwestern France (Néraudeau et al., 2010). This transgression corresponds to a high sea

183 level of +90m according to Hardenbol et al., (1998). The second transgression is mostly

184 characterized by the deposition of clays, which contains few bioclastic constituents

185 (Morzadec-Kerfourn, 1997, 1977). The so-called Redon clays formation are dated as

186 Pliocene: Piacenzian (Reuverian, ~2.7+/-0.3 Myr) from a pollen analysis (Morzadec-

187 Kerfourn, 1982, 1997). The corresponding sea level is around +60m according to the chart

188 (Hardenbol et al., 1998). The last known transgression in the area is characterized by clay

189 deposits that cover the Redon clays (Morzadec-Kerfourn, 1997). According to pollen analysis

190 of the Lanrinou clay at Landerneau (Morzadec-Kerfourn, 1982, 1997), these sediments can be

191 correlated with the lower Pleistocene around 1.6-2 Myr (Gelasian/Calabrian). The

192 corresponding event coincide with the high sea-level stand of +30m (Hardenbol et al., 1998).

193 Thus, at least three marine transgressions, with three different paleocoastlines, must be

194 considered for the Armorican massif: the oldest, which is also the highest, is Mio-Pliocene:

195 Messinian (~5.3+/-0.8 Myr) with sea level +90m asl, the second is Pliocene: Reuverian

196 (~2.7+/-0.3 Myr) with sea level +60m asl; and the most recent is Pleistocene:

197 Gelasian/Calabrian (~1.8+/-0.2 Myr) with sea level +30m asl.

198 Using local studies on the large-scale relief development and the paleotopographic evolution

199 of the Armorican basement (Bonnet et al., 1998, 2000; Brault et al., 2004; Guillocheau et al.,

200 2003; Lague et al., 2000; Lenôtre et al., 1999; Morzadec-Kerfourn, 1997; Van Vliet-Lanoe et

201 al., 1998), a paleotopography was reconstructed for the whole area.

202 Globally, the topography evolution is the result of tectonic movements, climate and eustatic

203 variations since the Mio-Pliocene. The modern topography is characterized by of incised

204 valleys with an incision average depth of 60-100m and significant topographic variations. The

205 onset of the current incised and dense hydrological network is probably not older than 1Ma

206 (Bonnet et al., 1998, 2000; Lefebvre et al., 1994). This topography contrasts with the smooth

207 planation surface of the Mio-Pliocene (Brault et al., 2004). The development of the

208 Pleistocene topography of the Armorican massif is explained by vertical movements due to

209 the N160 compression generated by the Alpine collision (Bonnet et al., 1998; Müller et al.,

210 1992; Nicolas et al., 1990). This differential tectonic uplift has been estimated from

211 geomorphological studies (Bonnet et al., 1998, 2000; Lague et al., 2000). Incision is measured

212 using a digital elevation model analysis. A distributed field of incised quantities is produced

213 for each individual drainage basin (Jost, 2005). Moreover, relief induced by fluvial incision

214 partly reflects continental movements and can be used to estimate uplift. Indeed, considering

215 that the drainage networks adjust to sea level, the induced incision has the same magnitude in

216 different basins. Thus the difference of incision is used to estimate the relative amounts of

217 differential uplift between basins. The estimation of differential uplift for each basin has been

218 grouped by zone due to the regional organization. A differential tectonic uplift has been

219 observed for the western part compared to the eastern part, along the Quessoy/Nort-sur-Erdre

220 fault (Brault et al., 2004; Jost, 2005).

221 From these previous work, to reconstruct the paleotopography of the whole area, we first used

222 a digital elevation model (DEM, 100m resolution) given by the Institut Géographique

223 National (IGN) to generate several surfaces providing an estimation of the Pleistocene

224 topography prior to erosion and valley incision (Bonnet et al., 1998, 2000). Within a

225 rectangular 20 km large sliding window, either the highest point or the Q90 quantile was

226 recorded. This process allows for the creation of a surface above the present-time topography

227 connecting the highest points and filling the valleys. The use of the Q90 quantile provides a

228 smoother result than the maximum which may be too influenced by isolated peaks. The

229 generated surface does not include the unknown amount of erosion of peaks and crests and

230 thus should be considered as a minimum. Then, the uplift (Jost, 2005) was subtracted from the

231 preprocessed topography. Last the paleocoastlines were reconstructed for the three

232 transgressions by comparing the reconstructed topography with the expected sea level derived

233 from Hardenbol et al., (1998). The Messinian and Reuverian transgressions had covered a

234 large part of the Armorican massif, except the highest elevations; the last Gelasian/Calabrian

235 transgression had flooded areas along the current coastline, and the lowest inland parts (Fig.

236 3).

237 **6. RESULTS**

238 **6.1. Origin of chlorides**

239 Within the framework of this study, 12 sites (monitoring sites in Fig. 2) presenting moderately

240 saline fluids (relative to the high chloride concentration) were subjected to further

241 geochemical and isotopic analysis (only Br concentrations are presented here) (Aquilina et al.,

242 2014). Salinities ranging from 60 to 1400mg/l were recovered at depths ranging from 41m to

243 200m, except for the Cinergy drilling project where water was collected at a depth below

244 450m in fractured schist, with a chloride concentration of 1240mg/l.

245 The chloride to bromide relationships is presented in Fig. 4 for the 12 sites investigated

246 geochemically. The chloride concentration is linearly correlated with bromide along the

247 rainfall-seawater mixing line (Fig. 4). This strongly suggests that the saline fluids in the

248 Armorican basement are of marine origin and correspond to paleoseawater diluted by

249   meteoric waters (Bottomley et al., 1994; Casanova et al., 2001; Frape et al., 1984; Fritz, 1997;

250   Gascoyne and Kamineni, 1994; Nordstrom et al., 1989).

251   Chloride has three potential sources: (1) (paleo)seawater, (2) rainfall potentially concentrated

252   by evapotranspiration processes, and (3) anthropogenic sources (agricultural fertilizers such as

253   KCl, pig slurry and cattle manure). If we exclude a 1-km band across the coastline, the

254   meteoric waters in Brittany have a maximum mean chloride concentration of 10-18mg.l^{-1} with

255   a relatively low variation range (Ayraud et al., 2008; Martin et al., 2004). Evapotranspiration

256   in Brittany represents about 50-60% of the total precipitation, and cannot provide chloride

257   concentrations in recharge water higher than 40 mg.l^{-1} (Ayraud et al., 2008). Agricultural

258   pollutions may increase the concentrations to 50mg.l^{-1} in the most intensively farmed areas

259   (Martin et al., 2004). Thus these two processes cannot explain the very high concentrations

260   observed. Furthermore a negative correlation between nitrate and altitude has been observed.

261   Above 100m, the nitrate concentration is almost constant and below 100m the nitrate

262   concentration decreases with depth. This negative correlation between nitrate and altitude

263   clearly as well as gas groundwater dating (Ayraud et al., 2008) indicates that below this depth

264   the anthropogenic influence decreases. These results underline that the anthropogenic sources

265   are more related to shallow aquifers, contrary to deep saline fluids. Many other sources of

266   chloride exist (as evaporitic deposits of geological formation…). But the relationships

267   between chloride and bromide will be completely different for evaporated brines or evaporite

268   leaching.

269   Thus, chloride concentrations are clearly out of the potential range of modern waters even

270   including anthropogenic sources. The correlation between bromide and chloride (Fig. 4)

271   supports a marine origin for these groundwater (Bottomley et al., 1994; Carpenter, 1978;

272   Freeman, 2007). The simplest mechanism which explains the high chloride concentration

273   observed is a marine component related to the last transgressions.

6.2. Spatial and vertical distributions of chloride

The chloride distribution is presented in Fig. 5 shows the altitudinal limits of the last three major transgressions between the Mio-Pliocene and the Pleistocene (Messinian ~5.3 Myr, Piacenzian ~2.7 Myr and Gelasian-Calabrian ~1.8 Myr). These limits correspond to 90, 60 and 30m, respectively. This map shows relatively high chloride concentrations (60 to 1400mg/L) around the current coastline and in a few large domains whose current topography is clearly above sea level. Only three zones present chloride concentrations below 40mg/L. These zones correspond to the three domains of higher elevation above 200m and to the area above the higher Messinian paleocoastline altitude of +90m asl. Fig. 6 shows the vertical distribution of chloride concentrations according to the altitude of the base of the well. Above 100m, the chloride concentration is almost constant, increasing only slightly with depth, the values ranging from 10 to 40mg/l. Below 100m, some drastic changes in the chloride-depth trends are observed. The main one is apparent at approximately 70m, with chloride concentrations up to 200 mg.l^{-1} observed below this depth. The chloride concentrations below 70m increase strongly with depth (approximately 0.5mg.l^{-1}.m^{-1} for the average and more than 1mg.l^{-1}.m^{-1} for the 90th percentile). This trend contrasts with the almost constant chloride concentrations in the areas not affected by past marine transgressions.

The distribution of chloride concentrations is in good agreement with the paleocoastlines (Fig. 5). The increase of chloride concentration with depth (Fig. 6) also supports this correlation. The vertical distribution of chloride concentrations likely indicates that, during each of the last transgressions, seawater was introduced by gravity-driven flow at great depth in the basement, and has only partially been flushed by meteoric waters.

6.3. The chloride releasing rate

The three paleocoastlines of past marine transgressions can be used to define four spatially distinct domains in the Armorican massif: three of them correspond to places where either the

Messinian, Reuverian and Gelasian/Calabrian transgressions is the last marine event that covered them; the fourth is the domain that was not flooded Fig. 5. The average chloride concentration for each area has been calculated and attributed to the age of the latest marine transgression. Fig. 7 shows that the average chloride concentration for each area is inversely related to the time elapsed since the last corresponding marine transgression.

This relationship shown in Fig. 7 can be fitted by a simple exponential function of the general form:

$$c = c_{in} \exp{-\frac{t_e}{\tau}} + c_o, \tag{1}$$

where c is the current chloride concentration, t_e is the age of the last transgression event, τ a characteristic time scale, c_o a background concentration, and c_{in} an additional concentration injected at the time t. Equation (1) is the solution of the differential equation:

$$\frac{dc}{dt} = -\frac{(c - c_o)}{\tau} + c_{in}\delta(t_e), \tag{2}$$

$\delta(t)$, the delta function, simulates quasi-instantaneous injection of chlorides at transgression times. The background chloride concentration c_o can be measured in places not influenced by past marine transgression; it is estimated to $21.5 \pm 0.3\,\mathrm{mg.l^{-1}}$. The regression fit leads to a time constant τ of 2.3 ± 0.1 Myr, and an injected concentration of $100 \pm 14\,\mathrm{mg.l^{-1}}$. The range errors for τ and c_{in} are calculated from the two regression fits generated from the errors on the dating methods used for each characteristic sediments and from the standard deviations of the current chloride concentration of each area. The envelope provided by the two regression fits shows the sensitivity of the parameters according to the standard errors. This residence-time order of magnitude is consistent with the residence time of several million years suggested by (Thury et al., 1994) for deep water as well as several studies supporting long residence times required by "fossil" seawater (Stober and Bucher, 1999). It can be noticed that these studies of fluids containing a paleoseawater end-member have chloride concentrations with an order of magnitude similar to those presented here.

14

7. DISCUSSION

7.1. General trend of increasing salinities with depth

The main results of this paper present clear evidences on the origin and the age of saline fluids in the continental crust at the scale of the Armorican massif. We report the vertical distribution of chloride concentration which presents a concentration increase with depth at the Armorican massif scale. Such a trend has already been observed in several places throughout the world in continental crust.

Highly saline brines have been found in various geological environments in the Canadian Shield (Frape et al., 1984; Fritz and Frape, 1982; Gascoyne and Kamineni, 1994), in the crystalline basement of Europe (Black Forest in Germany, Soultz-sous-forêt in France) (Aquilina et al., 1997; Pauwels et al., 1993; Stober and Bucher, 1999), in the Fennoscandian shield (Fritz, 1997; Nordstrom et al., 1989) and in the England Carnmenellis Granite (Edmunds et al., 1985). Saline fluids sampled in these sites report a wide range of chloride concentrations. At the surface, chloride concentration ranges from around ten to hundred mg/L, at much greater depth around 500m concentration values are between one hundred to thousands mg/L and below 1km depth concentrations range from hundreds to tens of thousands mg/L.

For all these sites chloride concentration have been analyzed by intervals of depth where the average chloride concentration is calculated in order to define the concentration gradient until approximately 1km of depth (Fig. 8). The Armorican data are also plotted on this graph (Fig. 8). All the studies show a general increase of salinity with depth. In the first three hundred meters a high gradient of salinity is observed and between 350 and about 700m, another gradient is observed. Below this depth, a stabilization seems to be observed although there are relatively few data (Fig. 8). However the main difference between all studies relies in chloride concentrations of groundwater samples at shallow depths. In fact, chloride concentration can

vary by one order of magnitude, with concentrations around ten to hundred mg/L, as for the

Armorican basement and the Canadian Shields, respectively (Fig. 8).

Previous studies (Aquilina et al., 1997; Edmunds et al., 1985; Frape et al., 1984; Fritz and Frape, 1982; Fritz, 1997; Gascoyne and Kamineni, 1994; Nordstrom et al., 1989; Pauwels et al., 1993; Stober and Bucher, 1999) have been realized in the framework of nuclear repository, geothermal or scientific programs with the aim to investigated the deep continental crust at depth ranging from several hundred meters to several kilometers. In this study we made a synthesis of a large number of wells in a much shallower part of the crystalline basement (41 to 200m). Despite the different purposes, we report similarities, specifically the distribution of chloride with depth which suggests common hydrogeological mechanisms. The salinity gradient from surface to greater depth and the smoothing of the evolution below a certain depth suggest two hydrodynamic behaviors. Such information can be useful to develop conceptual models of basement aquifers functioning. In addition, in this study we provide a time frame constraint of these processes in order to contribute to a better understanding.

7.2. Chloride releasing rate

Fig. 7 shows that the relationship between concentration and transgression age can be fitted by a decreasing exponential function, whose parameters give three different characteristics: the background concentration c_o which can be independently evaluated in places that have not been flooded by marine transgressions, c_{in} the additional concentration injected in the system during a transgression, and τ the "dilution" time scale. Note that even if the choice of the exponential function is rather arbitrary considering the small number of constraints, both c_{in}, the curve extrapolation for an event of age 0, and τ, the time to achieve a significant decrease, are rather well determined. However, it is also important to note that situation where three areas have been submerged successively by marine transgressions is exceptional. Even if, the three field-base data points makes for a weak fit, the contribution provides on the saline

372   fluids residence time is clearly better than all previous studies and consequently constitutes a

373   strong constraint. According to the fitting values, the average chloride concentration likely

374   increased by about 100mg.l^{-1} after each transgression. This is a rather low value compared to

375   the seawater concentration of ~19 g.l^{-1}, which indicates that the original seawater has replaced

376   only part of the freshwater initially present. During transgression, mechanism drives the

377   displacement of former fresh groundwater by seawater, but this process enables the saline

378   fluid circulation at great depth in fractured aquifers through the most permeable structures.

379   Nevertheless, all scales of porosity containing former fresh water are not directly influenced.

380   The presence of saline fluid in all scales of porosity requires the diffusion of saline fluid on

381   long term. Thus, the former fresh water already presents has a great contribution on the

382   injected concentration value and has a strong tendency to decrease the value. Then, the C_{in}

383   value estimated in our study is related to the entire volume of the aquifer which tends to

384   reduce the value. And, note that this value corresponds to the increase of the average chloride

385   concentration in the sampling zone that is mostly below 100 m of the current topography. If

386   there is a systematic increase of chloride concentration with depth, as observed in the upper

387   section, the average will increase as well. A deeper sampling could then give higher c_{in}

388   values. The fit also indicates that chloride flushing from the aquifers is a process requiring

389   approximately 2.3 Myr to return to initial conditions. The leaching process time constraints

390   the long-term hydrodynamics of Armorican aquifers but incorporates many environmental

391   conditions specific to the Armorican massif. Indeed, the efficiency of the leaching process is

392   influenced by numerous physical parameters and paleohydrologic conditions. One of the most

393   important parameter is the topographic gradient controlling gravitational flow and

394   consequently fluid migration. However, meteoric fluid migration into deeper parts of aquifer

395   depends on the hydrostratigraphic configuration of the region. The intensity of topography

396   driven flows is mainly controlled by geographic and climatic conditions. Changes in

397 topographic elevation due to tectonic and erosion processes also impact the behavior of flow

398 systems. In crystalline rock aquifers, as the Armorican basement, tectonic structures (faults

399 and fractures) play a major role through the formation of preferential pathways. Moreover, sea

400 level fluctuations can greatly influence topography driven fluid flow. In the case of an

401 important sea level modification, meteoric fluids may circulate deeper and induce mixing.

402 Thus, the characteristic residence time estimated in our study includes specific physical

403 parameters relating to the Armorican aquifers (geometry of the geological formations,

404 geomorphological features…) and all the changes caused by paleohydrologic conditions since

405 the seawater introduction (tectonic, erosion, sea-level fluctuations, climate changes…). While

406 taking account of the specified points and despite uncertainties on paleocoastlines and the

407 exponential function arbitrarily chosen, the essential point is the clear evidence of past marine

408 transgression during the last millions years and thus leaching processes being active during a

409 similar duration. We use these characteristic time of hydrodynamic processes to constraint the

410 conceptualization of basement aquifers functioning in the two next sections.

411 **7.3. Conceptualization of Armorican aquifers paleohydrogeology**

412 The Armorican massif presents clear evidences of a marine origin of the saline component in

413 the fluids at the massif scale. During marine transgression, seawater was introduced into the

414 basement by density-driven flow. This mechanism induced the displacement of former fresh

415 groundwater by seawater. Then due to diffusion process taking place on million year

416 (according to the time since transgression) the diffusion length scale (few hundred meters)

417 leads to a perfect mixing between marine waters and freshwaters already present in the whole

418 rock porosity. Third, following transgression, the marine signature contained in the system is

419 flushed out by groundwater circulations fed by meteoric waters. The preservation of marine

420 signature throughout the Armorican basement and the clear increase with depth support the

421 seawater introduction by gravity-driven flow at depth in the basement followed by a flushing

422   phase with limited downward fresh groundwater circulation loops. The flushing process leads

423   to the displacement of marine waters in the upper part of Armorican aquifers. The limited

424   depth of groundwater circulations is explained by the dense hydrological network, the high

425   sea-level and the low topography relief within the Armorican massif. Moreover, the chloride

426   releasing rate provides a time frame for the flushing process which has been estimated in the

427   order (of magnitude) of a few million years.

428   Such information can be used to develop conceptual models of the paleo-functioning of

429   Armorican aquifers. The objective of this section is thus to propose conceptual models that

430   may account for the chloride increase with depth on one hand and for the chloride

431   concentration increase fit with time presented above.

432   The crystalline basement of the Armorican massif presents aquifers with a high transmissivity

433   associated to fault zones (Roques et al., 2014). Considering the current topography of the

434   Armorican massif including three domains of higher elevation above 200m, the groundwater

435   flow system is driven gravitationally which leads to both local and regional circulation loops

436   (Toth, 1963). Considering the modern situation and constraints provided by the distribution of

437   chloride discussed previously, two main possibilities may explain the distribution of saline

438   fluids in Armorican aquifers.

7.3.1. First conceptual model: Perfectly mixed aquifer

440   First, the crystalline rock aquifers are considered as a perfectly mixed reactor where the time

441   constant of millions of years is also the residence time of chlorides in the system. The chloride

442   contained in the system is slowly flushed out by freshwater under the influence of

443   topography-driven groundwater flow (Toth, 1963). This model requires that chlorides are

444   located in a compartment of the groundwater system whose recharge is far lower than the

445   current recharge rate (around 200 mm.yr^{-1}) at the top boundary of the system (see Appendix

446   A). This does not necessarily means that this conceptual model is not consistent with data. On

447 the contrary, it seems consistent with the flow partitioning between local and regional flow

448 systems initially presented (Toth, 1963) and precised more recently (Cardenas, 2007;

449 Goderniaux et al., 2013). The characteristics of the partitioning between shallow aquifers and

450 deep aquifers have been studied using the topography of Brittany and assuming a constant

451 permeability with depth (Goderniaux et al., 2013). This study shows four interesting results

452 about the partitioning between shallow (short circulations related to first-order basins) and

453 deep (more regional circulations) aquifers: i) the "deep" compartment can be quite shallow

454 depending on local topography characteristics; ii) the residence time of particles is well fitted

455 by an exponential function, which means that the concentration flushing should behave

456 similarly; iii) the partitioning depends on the total recharge; (iv) the recharge flow in the deep

457 aquifer is 2-5 times smaller than the total recharge. These recharge values are not small

458 enough to explain the 2.3 Myr residence time observed for chlorides, which could mean either

459 that the first model is inconsistent with data, or that the assumption of Goderniaux et al.,

460 (2013) is unrealistic. A permeability decrease with depth, may observed in the continental

461 crust with a likely factor of 100 within the first kilometer (Ingebritsen and Manning, 1999;

462 Saar and Manga, 2004; Stober and Bucher, 2007). Such decrease could account for a much

463 smaller recharge of the deep groundwater system and thereby a flushing process less efficient.

464 Through modeling is ongoing to further test this hypothesis.

465   **7.3.2. Second conceptual model: Deep reservoir**

466 In the second case, the presumption is that chlorides could be localized in a deep reservoir i.e.

467 in the deeper part of the aquifer. Then chlorides would be leached out from the aquifer system

468 after diffusion from the deep reservoir towards the active part of the crystalline rock aquifers

469 where leaching is efficient. Calculations for this conceptual model (see Appendix A), lead to a

470 "salt" layer thickness of 40m that does not seem unrealistic as regards the chloride evolution

471 with depth observed. However this conceptual model would predict very high concentrations

472   at depth that are not yet observed in the Armorican basement in the absence of very deep

473   drillings. But, this could be in agreement with highly saline fluids sampled in various

474   geological environments at great depths worldwide (Fig. 8). As in the crystalline basement of

475   the Black Forest where Stober and Bucher (1999) suggest that the deep salt water discharges

476   is related to the upwelling of deep water which may bring up chloride from a deep reservoir.

477   However, it can certainly be affirmed that the salt contained in the deepest part is not solid

478   due to the chloride to bromide relationships which excludes this possibility.

479   The next step of this study will be to test these two functioning hypothesis with numerical

480   modeling in order to provide more realistic models. The objective is to provide some

481   constraints on the saline fluid circulation at the regional scale as well as to understand if the

482   heterogeneity and hydrodynamic conditions may induce a wide range of leaching rates which

483   could explain the large range of chloride concentrations observed.

484   **8. CONCLUSION**

485   Chloride concentrations in groundwater were investigated in the Armorican basement at

486   shallow depth (from +350 to -150masl). The high concentrations observed in some places

487   (from 60 to 1400mg/L) are shown to originate from marine transgressions. The distributions

488   of high chloride concentrations are in good agreement with both the altitudinal and vertical

489   limits and succession of the three major transgressions between the Mio-Pliocene and

490   Pleistocene ages. During each of the last transgressions, seawater was introduced by gravity-

491   driven flow at great depth in the basement. This seawater end-member has only partially been

492   flushed by meteoric waters (over 1 to 2 million years) between successive marine

493   transgressions, and since the last one. Considering the paleocoastlines, three zones have been

494   affected by the transgressions. The average chloride concentration calculated for each area is

495   inversely related to the time elapsed since last marine transgression. This relationship between

496   concentration and transgression age can be fitted by a decreasing exponential function which

497   indicates that chloride flushing from the aquifers is a process requiring approximately 2 Myr.

498   The fate of chloride is conceptualized using two main models: a dilution or leaching of a deep

499   reservoir. Both models provide information on the history of the saline fluids in fractured

500   aquifers. The first model requires a drastic partitioning between shallow and deep aquifers. In

501   the second model, chlorides are supposed to be released by diffusion from a deep reservoir,

502   leached by fresh groundwater flow and bringing up to the shallower aquifer. The model

503   supposes a deep reservoir, which has not yet been identified in the Armorican massif, but

504   could exist. This study thus provides important constraints on the seawater circulation in

505   hardrock aquifers at a continental-scale area.

506 **APPENDIX A**

507 The objective of this section is to develop simple calculations that aim at figuring out the

508 meaning of the data and fit presented before. We first assume that the average of chloride

509 concentrations measured is related to the average chloride concentration in the aquifer used in

510 the model. Because of the increase of chloride concentration with depth and because of the

511 limited sampling depth, it is unreasonable to pretend that the average of the measurements

512 equals the chloride average concentration in the entire aquifer. Thus, we just guess that the

513 chloride average in the entire aquifer evolves with a similar time scale to the measured

514 averages, which occur for instance if the depth dependency function is similar in different

515 places. Regardless of the model, the general evolution of the chloride concentration is given

516 by a mass balance equation of the type:

$$\frac{\mathbf{d}(V\bar{c})}{\mathbf{d}t} = -Q_c + Q_{in} \tag{3}$$

517 where V is the system volume, $\bar{c}$ the average chloride concentration in the system, Q_c the total

518 flow at the system discharge boundary, and Q_{in} the total flow at the system recharge

519 boundary. The "system" can be the entire aquifer or any part of it. Q_{in} represents a potential

520 chloride inflow from the recharge boundary. If we assume a background concentration c_o,

521 Q_{in} can be written as:

$$Q_{in} = \iint_{S_r} r(s).c_o \mathbf{d}s = c_o.A_r.\bar{r} \tag{4}$$

522 where S_r is the system recharge boundary, $r(s)$ the recharge at any point s of the boundary,

523 A_r the recharge boundary surface, and $\bar{r}$ the average recharge flow.

524 We then define two end-member models that may explain the chloride evolution in basement

525 aquifers.

526 **The perfectly mixed aquifer**

527   In the first model, the chloride contained in the deeper part of the aquifer is slowly flushed out

528   from the system along the discharge at a rate Q_c such as:

$$Q_c = \iint\limits_{S_d} q(s).c(s).\,\mathrm{d}s$$ (5)

529   where S_d is the system discharge boundary, $q(s)$ the flow discharge at any point s of the

530   boundary, and $c(s)$ the chloride concentration. In a perfectly-mixed reactor, the total

531   concentration at the boundary is equal to the concentrations average. Even if this

532   approximation is certainly unlikely in highly heterogeneous aquifers, we assume that the Q_c

533   integral can be estimated from the averages of concentrations and discharge Q_c defined as:

$$Q_c = O.A_d.\bar{q}.\bar{c}$$ (6)

534   where $\bar{q}$ and $\bar{c}$ are the discharge and concentration averages, respectively, and A_d is the total

535   surface of the system discharge boundary. $O(1)$ is a constant equal to 1 in the perfectly-mixed

536   approximation, and whose order of magnitude is about 1 if the approximation is not

537   rigorously exact. The water mass-balance requires that the total discharge equals the total

538   recharge: $A_d\bar{q} = A_r\bar{r}$. If we assume that the aquifer system is a rectangular box fed from

539   above with a recharge r, using a thickness $h = \frac{V}{A_r}$, equation ((3) writes as a first-order kinetic

540   equation :

$$\frac{\mathrm{d}\bar{c}}{\mathrm{d}t} = \frac{(c_o - O(1).\bar{c})}{\tau}$$ (7)

541   with the time constant τ equal to $\frac{h}{r}$.

542   If we consider that r is of the same order as it is now in Brittany (about 200mm.yr^{-1}), given

543   the time constant τ of 2.3 Myr, we predict an unrealistic aquifer depth h of about 500km.

544   Although the actual depth is not known, it is likely less than a few km and more likely about

545   1 km. This means that the dilution model is valid only if the recharge is at least 2 to 3 orders

546   of magnitude less than the current rainfall.

547 **The deep reservoir diffusion model**

548 In the second model, we assume that chlorides are leached out from the aquifer system by

549 diffusion from a deep layer of thickness h' without any advection. Q_c is a bit different from

550 equation (7) because diffusion occurs i) on all the system boundaries, and ii) at a rate equal to

551 $q(s) = D\frac{\partial c(s)}{\partial n}$, where n is the direction perpendicular to the system boundary. It is not easy

552 to estimate simply $q(s)$. We assume that the concentration gradient establishes in a length

553 scale of the order of the smallest aquifer dimension h', which is a reasonable assumption if

554 the aquifer thickness is small compared to its horizontal extent Q_c is defined as :

$$Q_c = O'.A.D.\frac{(\bar{c} - c_o)}{h'} \tag{8}$$

555 with O' an "order-of-magnitude" constant similar to O. The influx Q_{in} is now nil and the

556 general equation writes as:

$$\frac{d\bar{c}}{dt} = \frac{(c_o - \bar{c})}{\tau'} \tag{9}$$

557 with $\tau' = O'^{-1}.\frac{h'^2}{D}$.

558 The molecular diffusion D_m of chloride in water is of the order of 2.10^{-9} m^2.s^{-1} (Li and

559 Gregory, 1974; Wang et al., 1953). Considering a porosity of 1%, the diffusion D of chloride

560 is of the order of 2.10^{-11} m^2.s^{-1}. A time constant of 2.3 Myr is thus consistent with a salt layer

561 thickness of about 40 m.

562

566   **REFERENCES CITED**

567   Aquilina, L., Armandine Les Landes, A., Ayraud-Vergnaud, V., Labasque, T., Roques, C.,

568   Davy, P., Pauwels, H. and Petelet-Giraud, E.: Evidence for a Saline Component at Shallow

569   Depth in the Crystalline Armorican Basement (W France), Procedia Earth Planet. Sci., 7, 19–

570   22, doi:10.1016/j.proeps.2013.03.157, 2013.

571   Aquilina, L. and Dreuzy, J.-R. De: Relationship of present saline fluid with paleomigration of

572   basinal brines at the basement/sediment interface (Southeast basin – France), Appl.

573   Geochemistry, 26(12), 1933–1945, doi:10.1016/j.apgeochem.2011.06.022, 2011.

574   Aquilina, L., Pauwels, H., Genter, a. and Fouillac, C.: Water-rock interaction processes in the

575   Triassic sandstone and the granitic basement of the Rhine Graben: Geochemical investigation

576   of a geothermal reservoir, Geochim. Cosmochim. Acta, 61(20), 4281–4295,

577   doi:10.1016/S0016-7037(97)00243-3, 1997.

578   Aquilina, L., Vergnaud-Ayraud, V., Armandine Les Landes, A., Pauwels, H., Davy, P.,

579   PETELET-GIRAUD, E., Labasque, T., Roques, C., Bour, O., Ben Maamar, S., Kaskha, M.,

580   Le Gal La Salle, C., Barbecot, F. and Team, A.: Impact of climate changes during the last 5

581   million years on groundwaters in basement aquifers, PNAS, Submitted, 2014.

582   Ayraud, V., Aquilina, L., Labasque, T., Pauwels, H., Molenat, J., Pierson-Wickmann, A.-C.,

583   Durand, V., Bour, O., Tarits, C., Le Corre, P., Fourre, E., Merot, P. and Davy, P.:

584   Compartmentalization of physical and chemical properties in hard-rock aquifers deduced

585   from chemical and groundwater age analyses, Appl. Geochemistry, 23(9), 2686–2707,

586   doi:10.1016/j.apgeochem.2008.06.001, 2008.

587   Banks, D., Odling, N., Skarphagen, H. and Rohr-Torp, E.: Permeability and stress in

588   crystalline rocks, Terra Nov., 8(3), 223–235, 1996.

589   Beaucaire, C., Gassama, N. and Tresonne, N.: Saline groundwaters in the hercynian granites

590   (Chardon Mine, France): geochemical evidence for the salinity origin, Appl. Geochemistry,

591   14(1), 67–84, doi:10.1016/S0883-2927(98)00034-1, 1999.

592   Bonnet, S., Guillocheau, F. and Brun, J.: Large-scale relief development related to Quaternary

593   tectonic uplift of a Proterozoic-Paleozoic basement :, J. Geophys. Res., 105, 19,273–19,288,

594   2000.

595   Bonnet, S., Guillocheau, F. and Brun, J. P.: Relative uplift measured using river incisions: the

596   case of the armorican basement (France), Surf. Geosci., 327, 245–251, 1998.

597   Le Borgne, T., Bour, O., de Dreuzy, J. R., Davy, P. and Touchard, F.: Equivalent mean flow

598   models for fractured aquifers: Insights from a pumping tests scaling interpretation, Water

599   Resour. Res., 40(3), W03512, doi:10.1029/2003WR002436, 2004.

600   Le Borgne, T., Bour, O., Paillet, F. L. and Caudal, J.-P.: Assessment of preferential flow path

601   connectivity and hydraulic properties at single-borehole and cross-borehole scales in a

602   fractured aquifer, J. Hydrol., 328(1-2), 347–359, doi:10.1016/j.jhydrol.2005.12.029, 2006.

603   Bottomley, D. J., Gregoire, D. C. and Ravens, K. G.: Saline groundwaters and brines in the

604   Canadian Shield : Geochemical for a residual evaporite brine component and isotopic

605   evidence, Geochim. Cosmochim. Acta, 58(5), 1483–1498, 1994.

606 Bottomley, D. J., Katz, a., Chan, L. H., Starinsky, a., Douglas, M., Clark, I. D. and Raven, K.

607 G.: The origin and evolution of Canadian Shield brines: evaporation or freezing of seawater?

608 New lithium isotope and geochemical evidence from the Slave craton, Chem. Geol., 155(3-4),

609 295–320, doi:10.1016/S0009-2541(98)00166-1, 1999.

610 Brault, N.: Ressources du sous-sol et environnement en Bretagne. Génèse, géométrie et

611 propriétés de différents types d'aquifères, University of Rennes 1., 2002.

612 Brault, N., Bourquin, S., Guillocheau, F., Dabard, M.-P., Bonnet, S., Courville, P., Estéoule-

613 Choux, J. and Stepanoff, F.: Mio–Pliocene to Pleistocene paleotopographic evolution of

614 Brittany (France) from a sequence stratigraphic analysis: relative influence of tectonics and

615 climate, Sediment. Geol., 163(3-4), 175–210, doi:10.1016/S0037-0738(03)00193-3, 2004.

616 Bucher, K. and Stober, I.: Fluids in the upper continental crust, Geofluids, 10, 241–253,

617 doi:10.1111/j.1468-8123.2010.00279.x, 2010.

618 Cardenas, M. B.: Potential contribution of topography-driven regional groundwater flow to

619 fractal stream chemistry: Residence time distribution analysis of Tóth flow, Geophys. Res.

620 Lett., 34(5), L05403, doi:10.1029/2006GL029126, 2007.

621 Carpenter, A. B.: Origin And Chemical Evolution Of Brines In Sedimentary Basins, in SPE

622 Annual Fall Technical Conference and Exhibition, 1-3 October,., 1978.

623 Casanova, J., Negrel, P., Kloppmann, W. and Aranyossy, J. F.: Origin of deep saline

624 groundwaters in the Vienne granitic rocks (France): constraints inferred from boron and

625 strontium isotopes, Geofluids, 1(2), 91–101, doi:10.1046/j.1468-8123.2001.00009.x, 2001.

626 Chantraine, J., Egal, E., Thieblemont, D., Le Goff, E., Guerrot, C. and Ballevre, M.: The

627 Cadomian active margin (North Armorican Massif, France): a segment of the North Atlantic

628 Panafrican belt, Tectonophysics, 331, 1–18, 2001.

629 Clauser, C.: Permeability of crystalline rocks, Eos, Trans. Am. Geophys. Union, 73(21), 233–

630 238, 1992.

631 Le Corre, C., Auvray, B., Ballèvre, M. and Robardet, M.: Le Massif Armoricain, Sci. Geol.

632 Bull., 44, 31–103, 1991.

633 Dewandel, B., Lachassagne, P. and Wyns, R.: A generalized 3-D geological and

634 hydrogeological conceptual model of granite aquifers controlled by single or multiphase

635 weathering, J. Hydrol., 330(1-2), 260–284, doi:10.1016/j.jhydrol.2006.03.026, 2006.

636 Dorn, C., Linde, N., Doetsch, J., Le Borgne, T. and Bour, O.: Fracture imaging within a

637 granitic rock aquifer using multiple-offset single-hole and cross-hole GPR reflection data, J.

638 Appl. Geophys., 78, 123–132, doi:10.1016/j.jappgeo.2011.01.010, 2012.

639 Douglas, M., Clark, I. D., Raven, K. and Bottomley, D.: Groundwater mixing dynamics at a

640 Canadian Shield mine, J. Hydrol., 235(1-2), 88–103, doi:10.1016/S0022-1694(00)00265-1,

641 2000.

642 Dugué, O.: Le Massif Armoricain dans l'evolution Mésozoique et Cénozoique du Nord-Ouest

643 de l'Europe. Contrôles tectonique, eustatique et climatique d'un bassin intracratonique

644 (Normandie, Mer de la Manche, France), University of Caen., 2007.

645 Edmunds, W. ., Kay, R. L. F. and McCartney, R. .: Origin of saline groundwaters in the

646 Carnmenellis granite (Cornwall, England): Natural processes and reaction during hot dry rock

647 reservoir circulation, Chem. Geol., 49, 287–301, 1985.

648   Edmunds, W. . and Savage, D.: Geochemical Characteristics of Groundwater in Granites and

649   Related Crystalline Rocks., 1991.

650   Frape, S., Fritz, P. and Blackmer, A.: Saline groundwater discharges from crystalline rocks

651   near Thunder Bay, Ontario, Canada, Balanc. Freshw. Syst. [online] Available from:

652   http://iahs.info/redbooks/a150/150034.pdf (Accessed 15 March 2013), 1984.

653   Frape, S. K., Blyth, A., Blomqvist, R., McNutt, R. H. and Gascoyne, M.: Deep Fluids in the

654   Continents : II . Crystalline Rocks, p. 560., 2003.

655   Freeman, J. T.: The use of bromide and chloride mass ratios to differentiate salt-dissolution

656   and formation brines in shallow groundwaters of the Western Canadian Sedimentary Basin,

657   Hydrogeol. J., 15(7), 1377–1385, 2007.

658   Fritz, P.: Saline groundwater and brines in crystalline rocks: the contributions of John

659   Andrews and Jean-Charles Fontes to the solution of a hydrogeological and geochemical

660   problem, Appl. Geochemistry, 12(6), 851–856, doi:10.1016/S0883-2927(97)00074-7, 1997.

661   Fritz, P. and Frape, S. K.: Saline groundwaters in the Canadian Shield - A first overview,

662   Chem. Geol., 36, 179–190, 1982.

663   Gascoyne, M. and Kamineni, D. C.: The Hydrogeochemistry Of Fractured Plutonic Rocks In

664   The Canadian Shield, Hydrogeol. J., 2(2), 43–49, doi:10.1007/s100400050044, 1994.

665   Goderniaux, P., Davy, P., Bresciani, E., de Dreuzy, J.-R. and Le Borgne, T.: Partitioning a

666   regional groundwater flow system into shallow local and deep regional flow compartments,

667   Water Resour. Res., 49(4), 2274–2286, doi:10.1002/wrcr.20186, 2013.

668   Greene, S., Battye, N., Clark, I., Kotzer, T. and Bottomley, D.: Canadian Shield brine from

669   the Con Mine, Yellowknife, NT, Canada: Noble gas evidence for an evaporated Palaeozoic

670   seawater origin mixed with glacial meltwater and Holocene recharge, Geochim. Cosmochim.

671   Acta, 72(16), 4008–4019, doi:10.1016/j.gca.2008.05.058, 2008.

672   Gros, Y. and Limasset, O.: Déformation récente dans les socles cristallins. Exemple du Massif

673   Armoricain., 1984.

674   Guillocheau, F., Brault, N., Thomas, E., Barbarand, J., Bonnet, S., Bourquin, S., Estéoule-

675   Choux, J., Guennoc, P., Menier, D., Néraudeau, D., Proust, J.-N. and Wyns, R.: Histoire

676   géologique du Massif Armoricain depuis 140MA (Crétacé-Actuel)-Geological history of the

677   Armorican Massif since 140My (Cretaceous-Present Day), Bull. Inf., 40(1), 13–28, 2003.

678   Gumiaux, C., Gapais, D., Brun, J. P., Chantraine, J. and Ruffet, G.: Tectonic history of the

679   Hercynian Armorican Shear belt (Brittany, France), Geodin. Acta, 17, 289–307, 2004.

680   Hardenbol, J. A. N., Thierry, J., Farley, M. B., Cnrs, U. R. A. and Vail, P. R.: Mesozoic and

681   Cenozoic   sequence   chronostratigraphic   fremework   of   European   basins.   The

682   chronostratigraphic charts presented in this paper are the result of an initiative by Peter Vail

683   and Thierry Jacquin in 1990 to analyze and document depositional sequence, SEPM Spec.

684   Publ., (60), 3–13, 1998.

685   Ingebritsen, S. . and Manning, C. E.: Geological implications of a permeability-depth curve

686   for the continental crust, Geology, 27(12), 1107–1110, 1999.

687   Jost, A.: Caractérisation des forçages climatiques et géomorphologiques des cind derniers

688   millions d'années et modélisation de leurs conséquences sur un système aquifère complexe: le

689   bassin de Paris, University of Pierre and Marie Curie., 2005.

690   Kelly, V. R., Lovett, G. M., Weathers, K. C., Findlay, S. E. G., Strayer, D. L., Burns, D. J.

691   and Likens, G. E.: Long-Term Sodium Chloride Retention in a Rural Watershed: Legacy

692   Effects of Road Salt on Streamwater Concentration, Environ. Sci. Technol., 42(2), 410–415,

693   doi:10.1021/es0713911, 2008.

694   Lague, D., Davy, P. and Crave, A.: Estimating Uplift Rate and Erodibility from the Area-

695   Slope Examples from Brittany (France) and Numerical Modelling Relationship :, Phys.

696   Chem. Earth, 25(6-7), 543–548, 2000.

697   Larsson, I.: Les eaux souterraines des roches dures du socle: Projet 8.6 du Programme

698   Hydrologique International, 1987.

699   Lefebvre, D., Antoine, P., Auffret, J. P., Lautridou, J. P. and Lécolle, F.: Réponses de la Seine

700   et de la Somme aux événements climatiques, eustatiques et tectoniques du Pléistocène moyen

701   et récent : rythmes et taux d'érosion _ The responses of the river Seine and of the river

702   Somme to the climatic, eustatic and tectonic controls, Quaternaire, 5(3), 165–172,

703   doi:10.3406/quate.1994.2028, 1994.

704   Lenôtre, N., Thierry, P., Blanchin, R. and Brochard, G.: Current vertical movement

705   demonstrated by comparative levelling in Brittany (northwestern France), Tectonophysics,

706   301, 333–344, 1999.

707   Leray, S., de Dreuzy, J.-R., Bour, O. and Bresciani, E.: Numerical modeling of the

708   productivity of vertical to shallowly dipping fractured zones in crystalline rocks, J. Hydrol.,

709   481, 64–75, doi:10.1016/j.jhydrol.2012.12.014, 2013.

710   Li, Y.-H. and Gregory, S.: Diffusion of ions in sea water and in deep-sea sediments, Geochim.

711   Cosmochim. Acta, 38, 703–714, 1974.

712   Louvat, D., Michelot, J.-L. and Aranyossy, J. F.: Origin and residence time of salinity in the

713   Aspo groundwater system, Appl. Geochemistry, 14, 917–925, 1999.

714   Martin, C., Aquilina, L., Gascuel-Odoux, C., Molénat, J., Faucheux, M. and Ruiz, L.:

715   Seasonal and interannual variations of nitrate and chloride in stream waters related to spatial

716   and temporal patterns of groundwater concentrations in agricultural catchments, Hydrol.

717   Process., 18(7), 1237–1254, doi:ge, 2004.

718   Mercier, D., Brulhet, J., Beaudoin, B., Cahuzac, B., Laurent, M., Lauriat-Rage, A., Margerel,

719   J. P., Moguedet, G., Moritz, R., Sierra, P., Thiry, M., Turpin, L., Van Vliet-Lanoë, B. and

720   Vauthier, S.: Le Redonien de l'Ouest de la France : enregistrement des événements

721   (climatiques, eustatiques) messiniens et pliocènes sur la façade atlantique, 1res journées

722   GFEN-APF, 2000.

723   Morzadec-Kerfourn, M. T.: Datation pollinique et conditions de sédimentation de l'argile

724   plio-pléistocène de Lanrinou en Landerneau, Bull. l'Association française pour l'étude du

725   Quat., 19(4), 179–184, 1982.

726   Morzadec-Kerfourn, M. T.: Dinoflagellate cysts and the paleoenvironment of late Pliocene

727   early-Pleistocene deposits of Brittany, Quat. Sci. Rev., 16, 883–898, 1997.

728   Morzadec-Kerfourn, M.-T.: La limite Pliocene– Pleistocene en Bretagne, Boreas, 6, 275–283,

729   1977.

730   Mullaney, J. R., Lorenz, D. L. and Arntson, A. D.: Chloride in Groundwater and Surface

731   Water in Areas Underlain by the Glacial Aquifer System , Northern United States Scientific

732   Investigations Report 2009 – 5086., 2009.

733 Müller, B., Zoback, M. Lou, Fuchs, K., Mastin, L., Gregersen, S., Pavoni, N., Stephansson, O.

734 and Ljunggren, C.: Regional Patterns of Tectonic Stress in Europe, J. Geophys. Res., 97,

735 11,783–11,803, 1992.

736 Négrel, P. and Casanova, J.: Comparison of the Sr isotopic signatures in brines of the

737 Canadian and Fennoscandian shields, Appl. Geochemistry, 20(4), 749–766,

738 doi:10.1016/j.apgeochem.2004.11.010, 2005.

739 Négrel, P. and Pauwels, H.: Interaction between Different Groundwaters in Brittany

740 Catchments (France): Characterizing Multiple Sources through Strontium- and Sulphur

741 Isotope Tracing, Water, Air, Soil Pollut., 151(1-4), 261–285,

742 doi:10.1023/B:WATE.0000009912.04798.b7, 2004.

743 Néraudeau, D., Barbe, S., Mercier, D. and Roman, J.: Signatures paléoclimatiques des

744 échinides du Néogène final atlantique à faciès redonien, Ann. Paléontologie, 89(3), 153–170,

745 doi:10.1016/S0753-3969(03)00023-5, 2003.

746 Néraudeau, D., Dudicourt, J.-C., Boutin, F., Ceulemans, L. and Nicolleau, P.: Les Spatangus

747 du Miocène et du Pliocène de l'Ouest de la France, Ann. Paléontologie, 96(4), 159–170,

748 doi:10.1016/j.annpal.2011.05.001, 2010.

749 Néraudeau, D., Mercier, D., Van Vliet-Lanoë, B. and Lauriat-Rage, A.: Les faluns redoniens

750 stratotypiques, enregistrement partiel du Messinien atlantique, 1res journées GFEN-APF,

751 2002.

752 Nicolas, M., Santoire, J. P. and Delpech, P. Y.: Intraplate seismicity: new seismotectonic data

753 in Western Europe, Tectonophysics, 179(1-2), 27–53, doi:10.1016/0040-1951(90)90354-B,

754 1990.

755 Nordstrom, D. K., Olsson, T., Carlsson, L., Fritz, P., Survey, U. S. G., Road, M. and Park, M.:

756 Introduction to the hydrogeochemical investigations within the International Stripa Project*,

757 Geochim. Cosmochim. Acta, 53, 1717–1726, 1989.

758 Panno, S. V, Hackley, K. C., Hwang, H. H., Greenberg, S. E., Krapac, I. G., Landsberger, S.

759 and O'Kelly, D. J.: Characterization and identification of Na-Cl sources in ground water.,

760 Ground Water, 44(2), 176–87, doi:10.1111/j.1745-6584.2005.00127.x, 2006.

761 Pauwels, H., Aquilina, L., Negrel, P., Bour, O., Perrin, J. and Ahmed, S.: Groundwater

762 Salinization in Hard-Rock Aquifers: Impact of Pumping and Vertical Transfers, Procedia

763 Earth Planet. Sci., 7, 660–664, doi:10.1016/j.proeps.2013.03.189, 2013.

764 Pauwels, H., Ayraud-Vergnaud, V., Aquilina, L. and Molénat, J.: The fate of nitrogen and

765 sulfur in hard-rock aquifers as shown by sulfate-isotope tracing, Appl. Geochemistry, 25(1),

766 105–115, doi:10.1016/j.apgeochem.2009.11.001, 2010.

767 Pauwels, H., Fouillac, C. and Fouillac, A.: Chemistry and isotopes of deep geothermal saline

768 fluids in the Upper Rhine Graben: Origin of compounds and water-rock interactions,

769 Geochim. Cosmochim. Acta, 57, 2737–2749, 1993.

770 Perera, N., Gharabaghi, B. and Howard, K.: Groundwater chloride response in the Highland

771 Creek watershed due to road salt application: A re-assessment after 20years, J. Hydrol., 479,

772 159–168, doi:10.1016/j.jhydrol.2012.11.057, 2013.

773 Roques, C.: Hydrogeologie des zones de faille du socle cristallin : implications en terme de

774 ressources en eau pour le Massif Armoricain., 2013.

775 Roques, C., Bour, O., Aquilina, L., Dewandel, B., Leray, S., Schroetter, J., Longuevergne, L.,

776 Le Borgne, T., Hochreutener, R., Labasque, T., Lavenant, N., Vergnaud-Ayraud, V. and

777   Mougin, B.: Hydrological behavior of a deep sub-vertical fault in crystalline basement and

778   relationships with surrounding reservoirs, J. Hydrol., 509, 42–54, 2014.

779   Saar, M. O. and Manga, M.: Depth dependence of permeability in the Oregon Cascades

780   inferred from hydrogeologic, thermal, seismic, and magmatic modeling constraints, J.

781   Geophys. Res., 109(B4), B04204, doi:10.1029/2003JB002855, 2004.

782   Starinsky, A. and Katz, A.: The formation of natural cryogenic brines, Geochim. Cosmochim.

783   Acta, 67(8), 1475–1484, doi:10.1016/S0016-7037(02)01295-4, 2003.

784   Stober, I. and Bucher, K.: Deep groundwater in the crystalline basement of the Black Forest

785   region, Appl. Geochemistry, 14(2), 237–254, doi:10.1016/S0883-2927(98)00045-6, 1999.

786   Stober, I. and Bucher, K.: Hydraulic properties of the crystalline basement, Hydrogeol. J.,

787   15(2), 213–224, doi:10.1007/s10040-006-0094-4, 2007.

788   Stober, I., Richter, A., Brost, E. and Bucher, K.: The Ohlsbach Plume – Discharge of deep

789   saline water from the crystalline basement of the Black Forest, Germany, Hydrogeol. J., 7(3),

790   273–283, doi:10.1007/s100400050201, 2002.

791   Thomas, E.: Evolution Cenozoique d'un domaine de socle: Le Massif Armoricain., 1999.

792   Thury, M., Gautschi, A., Mazurek, M., Müller, W. H., Naef, H., Pearson, F. J., Vomvoris, S.

793   and Wilson, W.: Geology and Hydrogeology of the Crystalline Basement of Northern

794   Switzerland. Synthesis of Regional Investigations 1981-1993 within the Nagra Radioactive

795   Waste Disposal Programme. Nagra, Technical Report., 1994.

796   Toth, J.: A theoretical analysis of groundwater flow in small drainage basins, J. Geophys.

797   Res., 68, 4795–4812, 1963.

798   Touchard, F.: Caractérisation hydrogéologique d'un aquifère de socle fracturé : site de

799   Ploemeur (Morbihan)., 1999.

800   Van Vliet-Lanoe, B., Laurent, M., Hallégouët, B., Margerel Jean-pierre, Chauvel, J., Michel,

801   Y., Moguedet, G., Trautman, F. and Vauthier, S.: Le Mio-Plioche du Massif armoricain.

802   Données nouvelles_ The Mio-Pliocene of the Armorican Massive. New data, Surf. Geosci.,

803   326, 333–340, 1998.

804   Wang, J. ., Robinson, C. . and Edelman, I. .: Self diffusion and structure of liquid water with

805   2H, 3H and 18O as tracers, J. Am. Chem. Soc., 75, 466–470, 1953.

806   Wyns, R., Baltassat, J., Lachassagne, P. and Legchenko, A.: Application of proton magnetic

807   resonance soundings to groundwater reserve mapping in weathered basement rocks, Bull.

808   société géologique Fr., 21–34, 2004.

809   Ziegler, P. A.: Geological atlas of Western and Central Europe, in Mesozoic and Cenozoic.,

810   1990.

811

812

813   FIGURE CAPTIONS

814
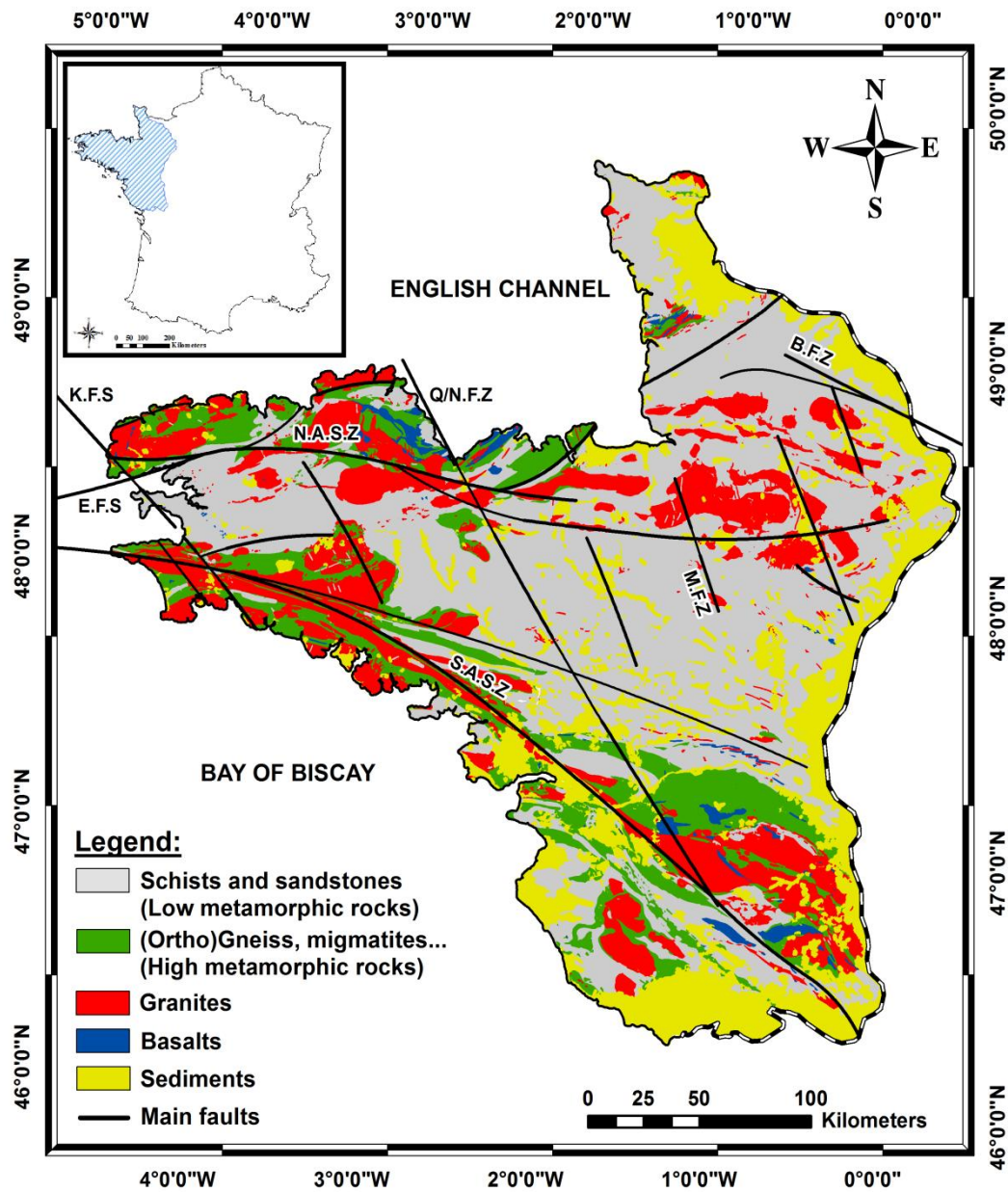
Fig. 1. Simplified geological map of the main lithological units and main geological structures of the Armorican Massif: NASZ: North Amorican Shear Zone; SASZ: South Armorican Shear Zone; Q/NFZ: Quesssoy/Nort-sur-Erdre Fault Zone; MFS: Mayenne fault System; KFS: Kerforne Fault System and EFS: Elorne Fault system (according to Bonnet et al. 2000).
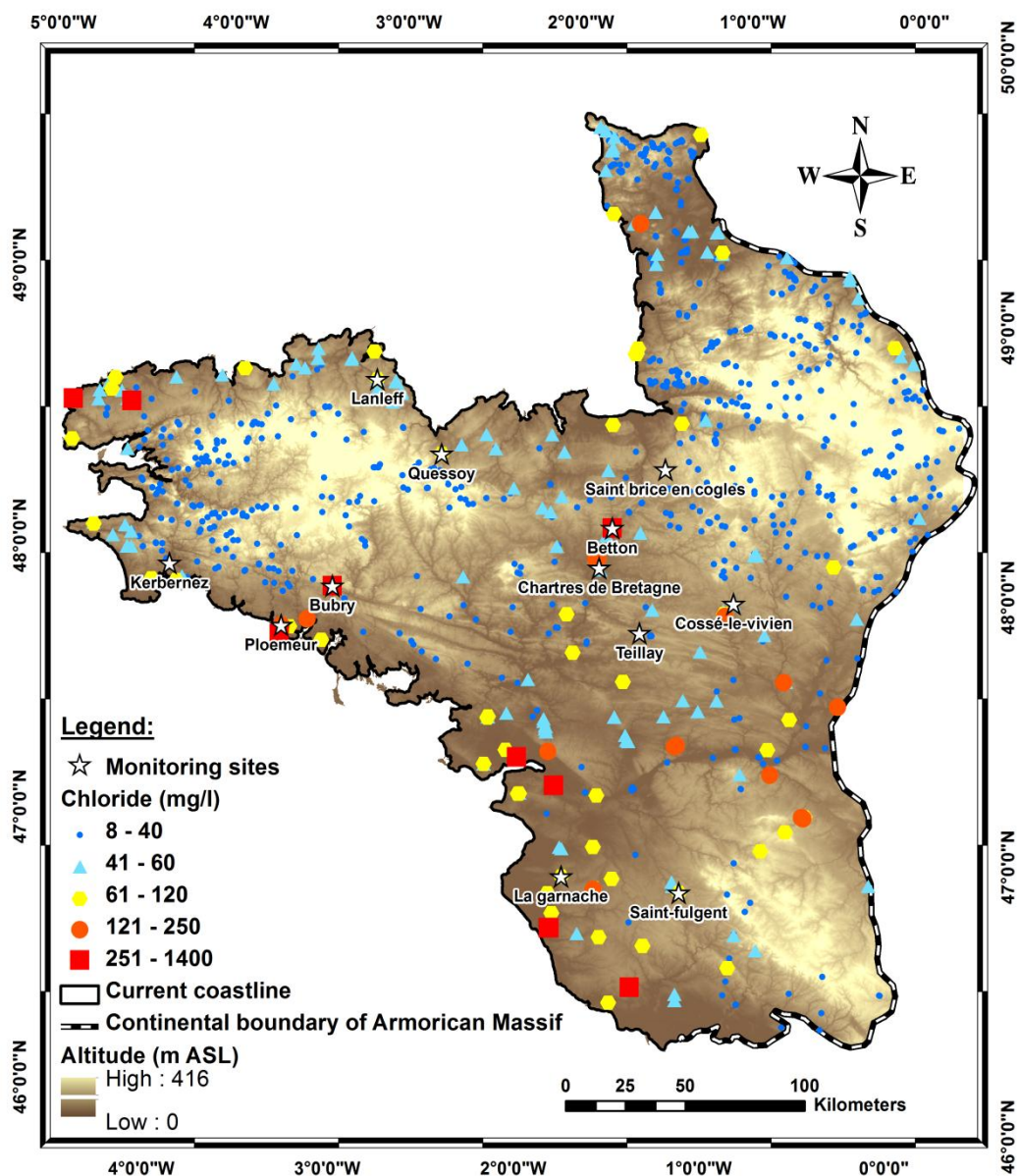
819

820

Fig. 2. Map of the Armorican Massif including the distribution of chloride concentration for the whole area (from preprocessed chloride database) and the location of the 12 sites investigated.

823
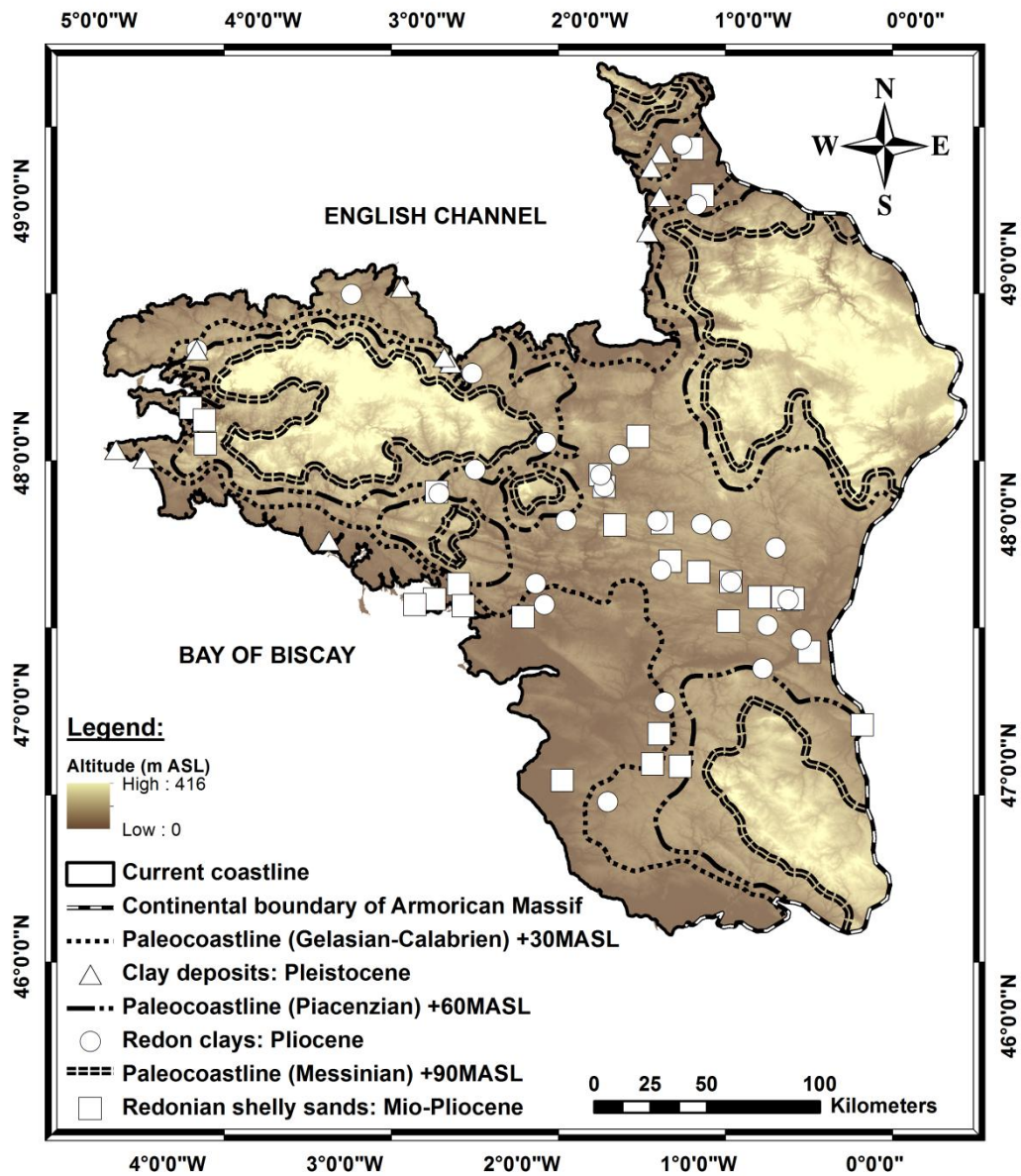
Fig. 3. Localization of paleocoastlines on the current topography for past marine transgressions since the Mio-Pliocene time and characteristic sediments associated for each flooding period.
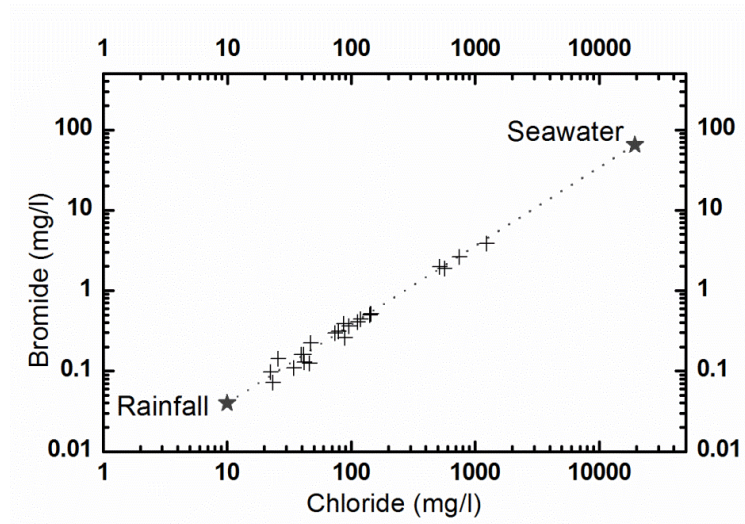
826

Fig. 4. Br versus Cl concentrations of groundwater in the 12 sites investigated.
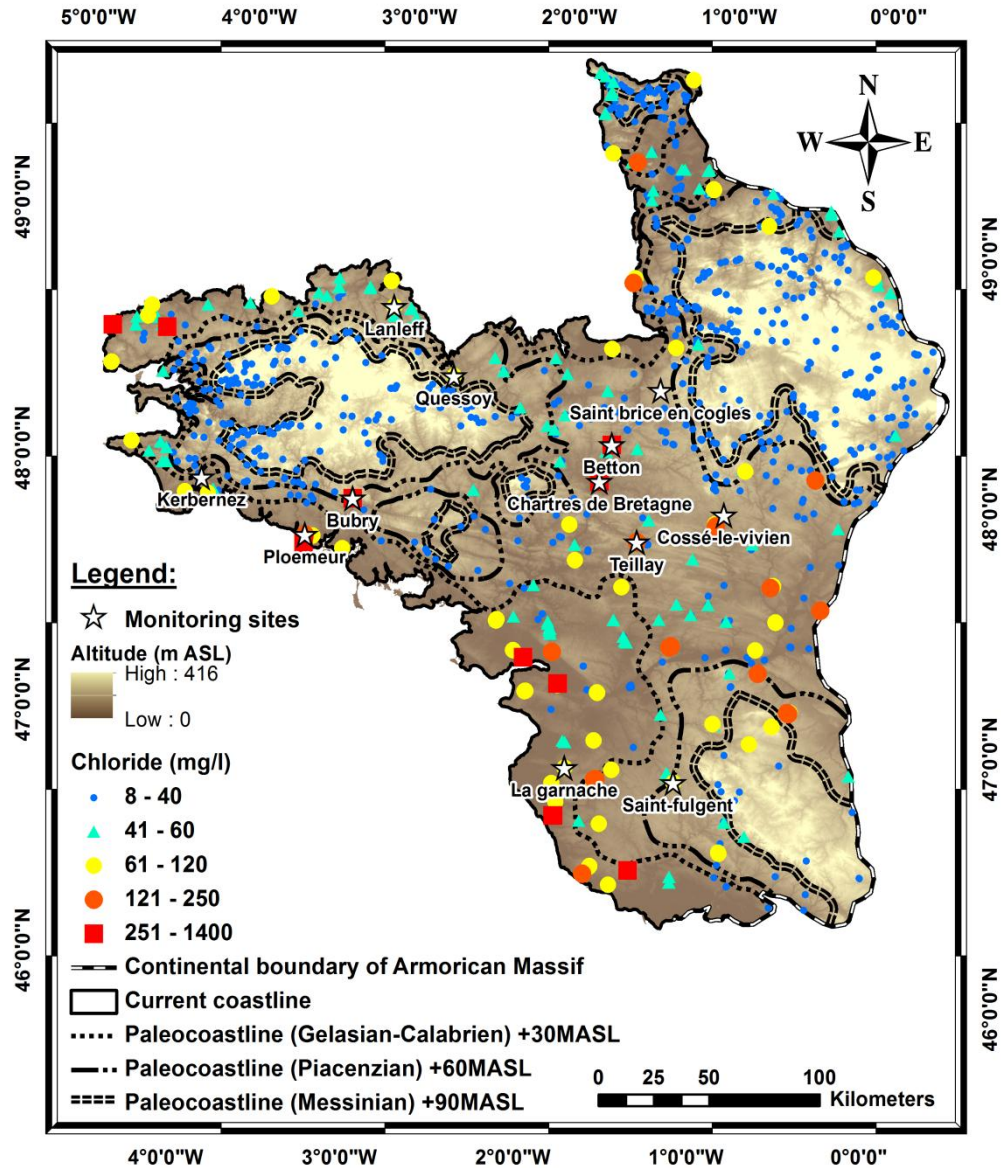
828

829

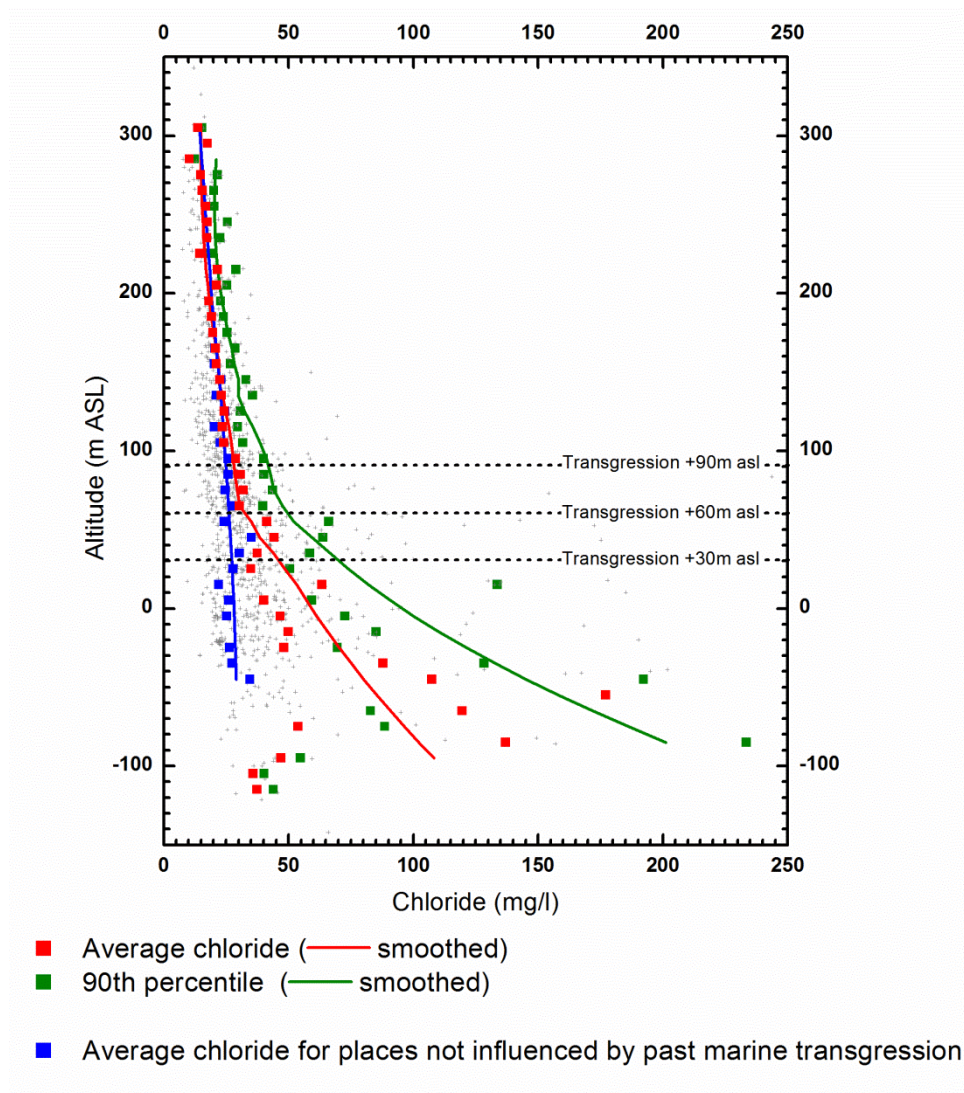830   **Fig. 5. Distribution of paleocoastlines on the current topography for the three transgressions.**

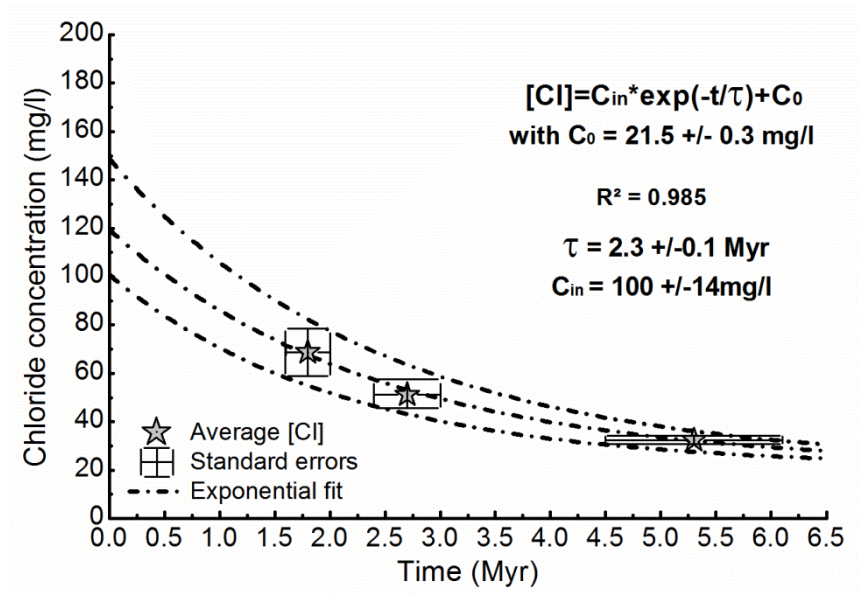Fig. 6. Chloride concentrations versus altitude of well base.

831

832

$$[Cl]=C_{in}*exp(-t/\tau)+C_0$$

with $C_0 = 21.5$ +/- 0.3 mg/l

$R^2 = 0.985$

$\tau = 2.3$ +/-0.1 Myr

$C_{in} = 100$ +/-14mg/l

☆ Average [Cl]
⊞ Standard errors
–·– Exponential fit

833

834   **Fig. 7. Average chloride concentration for each transgression zone versus the elapsed time since the transgression.**
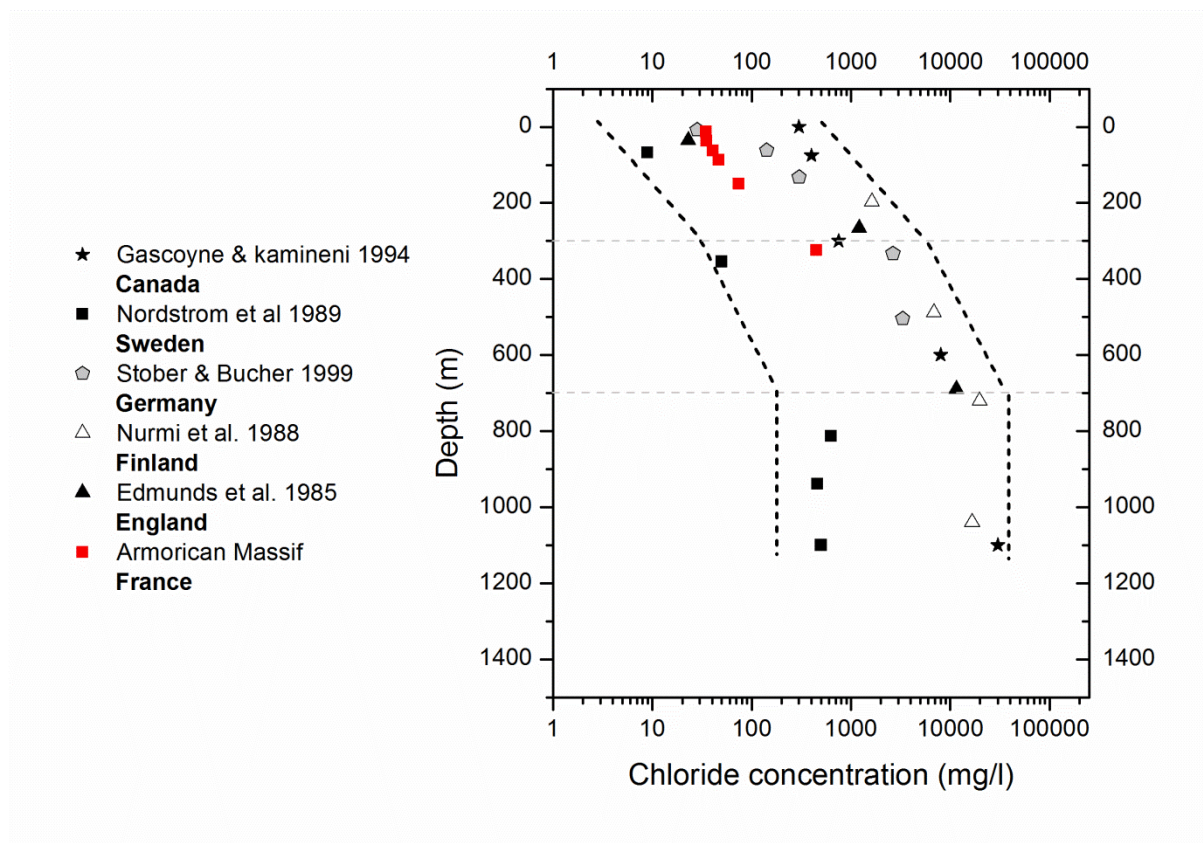
835

836

Fig. 8. Chloride concentration (mg/l) versus depth (m) recorded in continental basement around the world compared with the data of the current study.